Averaging method of granular materials

H. P. Zhu and A. B. Yu*

*Centre for Computer Simulation and Modelling of Particulate Systems, School of Materials Science and Engineering,
The University of New South Wales, Sydney, New South Wales 2052, Australia*

This paper presents an averaging method to link discrete to continuum variables of granular materials. Compared to the other methods proposed in the literature, it has advantages of being applicable to all flow regimes, and to granular flows with or without the effect of physical boundaries. Its application is demonstrated in the determination of the macroscopic properties such as mass density, velocity, stress, and couple stress distributions of a hopper flow, where the discrete results are generated by means of discrete particle simulation. While highlighting the need for considering properly the effect of physical boundaries, the results indicate that the proposed method is an effective way to determine the flow properties of granular materials.

I. INTRODUCTION

Granular materials, which can be either wet or dry and range in size from nanometers to centimeters, are widely encountered in industries and in nature. As with solids, they can withstand deformation and form heaps; as with liquids, they can flow; as with gases, they exhibit compressibility. These features give rise to another state of matter that is poorly understood [1,2]. This can be highlighted from the study of granular flow—the area concerned in this work. Corresponding to the fluidlike and solidlike modes, different regimes have been identified in the past: quasistatic regime, rapid flow regime, and a transitional regime that lies in between. However, development of a general theory to describe granular flow has still been a challenging problem (see Ref. [3], for example).

Essentially, the existing approaches to granular flow can be classified into two categories: the continuum approach at a macroscopic level and the discrete approach at a microscopic level. In the continuum approach, the macroscopic behavior of granular flow is described by the balance equations facilitated with constitutive relations and boundary conditions. The most difficult problem in implementing this approach lies in the determination of suitable constitutive relations. In the past, different theories have been devised for different materials and for different flow regimes. For example, models have been proposed to derive the constitutive equations for the rate-independent deformation of granular materials based on either the plasticity theory or the double shearing theory [4–6]; rapid flow of granular materials has been described by extending the kinetic theory of dense gases [7,8]; the transitional regime that involves both collisional and frictional mechanisms is studied by use of the kinetic theory combined with the Mohr-Coulomb quasistatic theory [9]. However, to date, there is no accepted continuum theory applicable to all flow conditions.

The discrete approach is based on the analysis of the motion of individual particles and has the advantage that there is no need for global assumptions on the solids such as steady-state behavior, uniform constituency, and/or constitutive relations. A major type of discrete approach is based on the so-called distinct element method (DEM) originally developed by Cundall [10] for rock mechanics or its extended version applied to granular materials [11]. The method considers a finite number of discrete particles interacting by means of contact and noncontact forces, and every particle in a considered system is described by Newton's equations of motion related to translational and rotational motions. DEM-based simulation has been recognized as an effective method to study the fundamentals of granular materials (see Ref. [12], for example). However, it is difficult to adapt this approach to process modeling because of the limited particle numbers which can be handled with the present computing capacity.

Extensive research has been carried out to develop an averaging theory to link the microscopic variables in the discrete approach to the macroscopic variables in the continuum approach. Drescher and de Josselin de Jong [13] first suggested a volume averaging method to define the stress tensor where the average stress of an assembly of particles with arbitrary shape is expressed in terms of the external forces acting at the boundary points of the assembly. Rothenburg and Selvadurai [14], Christoffersen, Mehrabadi, and Nemat-Nasser [15], and Kanatani [16], respectively, proposed different average equations based on different theoretical considerations. Under the conditions of equilibrium, the equations proposed by these authors are actually equivalent to each other. The key feature of the treatments involved is that the stress tensor is expressed in terms of individual contact forces within an assembly of particles, and the inertial terms are neglected. This volume averaging technique, often with some modifications, has been used by various investigators to study the strain tensor and stress-strain relationship under various flow conditions [17–24]. The micromechanical definition of couple stress has also been considered in some recent studies (see Refs. [4,22–24], for example). In particular, the models of Lätzel, Luding, and Herrmann [22,23] and Luding [24] included more macroscopic characteristics such as volume fraction and fabric tensor. Walton and Braun [25,26] proposed an alternative method based on time-volume averaging in their study of a rapid granular flow, which was later improved by Zhang and Campbell [27]

---

*Corresponding author, Fax: +61 2 9385 5956. Email address: a.yu@unsw.edu.au

and Campbell [28,29] to include a couple stress term.

The above methods have been applied to the dynamical analysis of granular flows (e.g., Langston, Tüzün, and Heyes [30] and Potapov and Campbell [31]). However, some restrictive assumptions have to be employed in these models, which limit their general application. For example, to a large degree, the volume averaging approach is valid for quasistatic systems because the inertial effect is ignored and a static equilibrium condition is used. Although the time-volume averaging has been demonstrated to be applicable to simple shear rapid flows, its applicability to other granular flows has been questionable [32]. In recent years, various attempts have been made to develop a more general averaging method [33–37]. Of particular interest is the weighted time-space averaging method presented by Babic [32], which has been verified to be fully compatible with the kinetic theory of rapid granular flows [33] and extended to study the constitutive behavior of granular materials [35,36]. The weighted time-space averaging method has two main advantages. First, the macroscopic quantities obtained conform with those in the common balance equations in the continuum approach so that they have clear physical meaning. Second, it is in principle applicable to both solidlike and fluidlike modes of granular materials. However, difficulties may arise in the application of Babic's method. For example, the method thus far developed is only valid within the domain far from the boundaries of a granular system, not applicable to practical systems, e.g., granular flow in a hopper or any process vessel in industry, where physical boundaries are present and may affect granular flow significantly. In addition, the weighting function used for averaging should be more constrained so that the resultant macroscopic quantities satisfy fully the conditions in the continuum mechanics such as the continuity in a considered domain.

In this paper, we present modified average equations to overcome these problems in connection with our earlier attempt where the rational motion of particles is ignored [37]. We first develop average equations which are valid for the entire domain including the interior and physical boundaries of granular material and applicable to all flow regimes, and propose a weighting function. Then, we carry out DEM simulation of granular flow in a cylindrical hopper with flat bottom and obtain, by means of the proposed averaging method, its macroscopic quantities such as mass density, velocity, stress, and couple stress distributions based on the discrete results.

II. AVERAGING METHOD

A. Discrete system and its balance equations

In general, a granular system is composed of discrete particles, and every particle in the system can be described by Newton's equations of motion. If possible mass transfer between particles, say, due to chemical reactions, is not considered, the mass of every particle is constant, so that for particle i,

$$\frac{d}{dt} m_i = 0. \tag{1}$$

The equations for translational and rotational motion and energy for this particle can be generally written as

$$\frac{d}{dt}(m_i \mathbf{v}_i) = \sum_j \mathbf{f}_{ij} + \mathbf{f}_i^b + m_i \mathbf{g}, \tag{2}$$

$$\frac{d}{dt}(\mathbf{l}_i \cdot \boldsymbol{\omega}_i) = \sum_j \mathbf{m}_{ij} + \mathbf{m}_i^b, \tag{3}$$

$$\frac{d}{dt} E_i = \sum_j (W_{ij} + Q_{ij}) + W_i^b + Q_i^b + W_i^g + H_i. \tag{4}$$

Equations (2) and (3) have extensively been used in DEM [11,12] whilst Eq. (4) is an extension version of Babic [32] to take into account the effect of physical boundaries. The quantities in these equations are explained in Table I. Summation over j can extend over all particles in the system, although often limited to particles adjacent to particle i. The forces between particle i and other particles and boundaries include the short-range contact forces and the long-range noncontact forces such as van der Waals and electrostatic forces. The torques acting on the particle include those arising from the tangential forces and the rolling resistance. The energy of particle i generally consists of intrinsic energy ε_i and kinetic energy K_i, so that $E_i = \varepsilon_i + K_i$, where $K_i = \frac{1}{2}(m_i \mathbf{v}_i \cdot \mathbf{v}_i + \boldsymbol{\omega}_i \cdot \mathbf{l}_i \cdot \boldsymbol{\omega}_i)$. The rates of mechanical work done by the body force on the particle is $W_i^g = m_i \mathbf{g} \cdot \mathbf{v}_i$.

For convenience, let $\mathbf{X}_i = (m_i, m_i \mathbf{v}_i, \mathbf{l}_i \cdot \boldsymbol{\omega}_i, E_i)$ denote the vector of the physical quantities in the left side of above equations, and $\mathbf{P}_{ij} = (0, \mathbf{f}_{ij}, \mathbf{m}_{ij}, W_{ij} + Q_{ij})$, $\mathbf{B}_i = (0, \mathbf{f}_i^b, \mathbf{m}_i^b, W_i^b + Q_i^b)$ and $\mathbf{G}_i = (0, m_i \mathbf{g}, \mathbf{0}, W_i^g + H_i)$. Then, the above equations can be generally written as

$$\frac{d}{dt} \mathbf{X}_i = \sum_j \mathbf{P}_{ij} + \mathbf{B}_i + \mathbf{G}_i. \tag{5}$$

This equation gives a full description of granular flow at a particle scale and is hence used in the following discussion.

B. Continuum system and its balance equations

By use of a proper weighting technique, the discrete system considered above can be transferred into a continuum system. In this work, the weighting function involved is denoted as $h(\mathbf{r}, t)$, where $\mathbf{r} = (x, y, z)$ represents the position coordinates. $h(\mathbf{r}, t)$ is positive in the limited domain $\Omega = \{(\mathbf{r}, t) | \mathbf{r} \in \Omega_p \subset R^3, t \in T = [T_0, T_1] \subset R\}$; otherwise, zero. The function should satisfy the condition of normalization, i.e., $\int_{R^4} h(\mathbf{r}, t) d\mathbf{r}\, dt = 1$. Then, the local average of the physical property $\mathbf{X}_i$ can be defined by use of $h(\mathbf{r}, t)$. There are two types of cells for averaging: interior cells which are located far from boundaries and exterior cells which are close to a boundary, as demonstrated in Fig. 1. The local average of physical property $\mathbf{X}_i$ at a point $\mathbf{r}$ and a time t corresponding to interior cells can be generally written as

$$\bar{\mathbf{X}}(\mathbf{r}, t) = \int_{T_t} \sum_i h_i \mathbf{X}_i(s) ds, \tag{6}$$

TABLE I. Quantities in the balance equations of discrete system and continuum system.

Discrete system		Continuum system[a]	
m_i	Mass of particle i	ρ	Mass density
$\mathbf{v}_i$	Velocity of particle i	$\mathbf{u}$	Velocity
$\boldsymbol{\omega}_i$	Angular velocity of particle i	$\boldsymbol{\omega}$	Angular velocity
$m_i\mathbf{v}_i$	Linear momentum of particle i	$\mathbf{l}\cdot\boldsymbol{\omega}$	Internal spin density
$\mathbf{l}_i\cdot\boldsymbol{\omega}_i$	Angular momentum of particle i	$\mathbf{T}$	Stress tensor
$\mathbf{f}_{ij},\,\mathbf{f}_i^b$	Interaction forces acting on particle i exerted by particle j and boundary	$\mathbf{M}$	Couple stress tensor
$\mathbf{g}$	Body force per unit mass acting on particle	$\mathbf{M}'$	Rate of supply of internal spin to particles
$\mathbf{m}_{ij},\,\mathbf{m}_i^b$	Torques acting on particle i exerted by particle j and boundary	E	Energy density
E_i	Energy of particle i	$\mathbf{q}^E$	Total flux of kinetic energy and intrinsic energy
$W_{ij},\,W_i^b,\,W_i^g$	Rates of mechanical work done by particle j, the boundary, and the body force on particle i	h	Heat source density
$Q_{ij},\,Q_i^b$	Rates of heat transfer from particle j and boundary to particle i		
H_i	Heat source of particle i		

[a]In this work, the effect of physical boundary is included in the above macroscopic quantities.

where $T_t=[T_0+t,T_1+t]$, $h_i=h(\mathbf{r}_i-\mathbf{r},s-t)$; and for exterior cells, it is defined as

$$\bar{\mathbf{X}}(\mathbf{r},t)=\int_{T_t}\sum_i g_i\mathbf{X}_i(s)ds, \tag{7}$$

where $g_i=g(\mathbf{r}_i-\mathbf{r},s-t)$, $g(\mathbf{r}'-\mathbf{r},s-t)=h(\mathbf{r}'-\mathbf{r},s-t)$ $+h(\mathbf{r}''-\mathbf{r},s-t)$ for $\mathbf{r}'\in R^3$, $\mathbf{r}_i''$ is the symmetric point of $\mathbf{r}_i'$ with respect to the contacting boundaries. It can be shown that $g(\mathbf{r}'-\mathbf{r},s-t)$ satisfies the condition of normalization $\int_{R^4}g(\mathbf{r}'-\mathbf{r},s-t)d\mathbf{r}'dt=1$. In connection with Eq. (6), Eq. (7) can be rewritten as

$$\bar{\mathbf{X}}(\mathbf{r},t)=\int_{T_t}\sum_i h_i\mathbf{X}_i(s)ds$$

$$\triangleq\int_{T_t}\sum_i h(\mathbf{r}_i'-\mathbf{r},s-t)\mathbf{X}_i(s)ds$$

$$+\int_{T_t}\sum_i h(\mathbf{r}_i''-\mathbf{r},s-t)\mathbf{X}_i(s)ds. \tag{8}$$
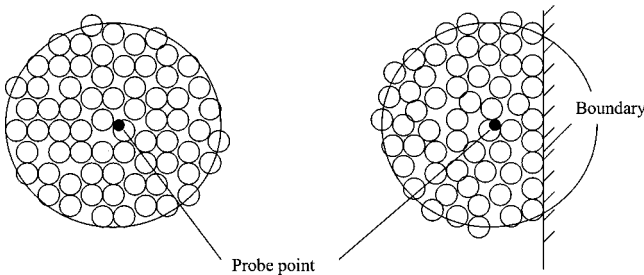
FIG. 1. A two-dimensional schematic illustration of the concepts of probe point, and interior and exterior cells.

$\bar{\mathbf{X}}(\mathbf{r},t)$ can give the local averages of mass, linear momentum, angular momentum, and energy, which are commonly used in the continuum description of granular flow (please refer to Table I). Let $\bar{\mathbf{X}}(\mathbf{r},t)=(\rho,\rho\mathbf{u},\rho\mathbf{l}\cdot\boldsymbol{\omega},\rho E)$, and define respectively ρ and $\mathbf{l}$ as

$$\rho=\int_{T_t}\sum_i h_i m_i ds \tag{9}$$

and

$$\mathbf{l}=\frac{1}{\rho}\int_{T_t}\sum_i h_i\mathbf{l}_i ds. \tag{10}$$

According to Eq. (6), we have

$$\mathbf{u}=\frac{1}{\rho}\int_{T_t}\sum_i h_i m_i\mathbf{v}_i ds, \tag{11}$$

$$\boldsymbol{\omega}=\frac{1}{\rho\mathbf{l}}\int_{T_t}\sum_i h_i\mathbf{l}_i\cdot\boldsymbol{\omega}_i ds, \tag{12}$$

$$E=\frac{1}{\rho}\int_{T_t}\sum_i h_i E_i ds. \tag{13}$$

The instantaneous velocity $\mathbf{v}_i$ of particle i can be decomposed into an average part $\mathbf{u}$ and a fluctuating part $\mathbf{v}_i'$, so that $\mathbf{v}_i=\mathbf{u}+\mathbf{v}_i'$. Similarly, for the instantaneous angular velocity $\boldsymbol{\omega}_i$, we have $\boldsymbol{\omega}_i=\boldsymbol{\omega}+\boldsymbol{\omega}_i'$, and consequently the energy density $E=K+K'+U$, where K is the kinetic energy density, K' is the fluctuating kinetic energy density, and U is the intrinsic energy density. K, K', and U can be expressed as

$$K = \tfrac{1}{2}(\mathbf{u}\cdot\mathbf{u} + \boldsymbol{\omega}\cdot\mathbf{l}\cdot\boldsymbol{\omega}), \tag{14}$$

$$K' = \frac{1}{2\rho}\int_{T_t}\sum_i h_i(m_i\mathbf{v}_i'\cdot\mathbf{v}_i' + \boldsymbol{\omega}_i'\cdot\mathbf{l}_i\cdot\boldsymbol{\omega}_i')ds, \tag{15}$$

$$U = \frac{1}{\rho}\int_{T_t}\sum_i h_i\varepsilon_i ds. \tag{16}$$

Now to develop balance equations for the continuum system on this basis, we follow the treatment of Savage [38]. Suppose that L is an element of the system, associated with volume $d\tau_0 = dx\,dy\,dz$ containing point $\mathbf{r}$. Then, $\mathbf{A}(\mathbf{r},t) = \bar{\mathbf{X}}(\mathbf{r},t)d\tau_0$ designates the mass, linear momentum, angular momentum, and energy of this element. We can derive an expression of the material derivative of $\mathbf{A}(\mathbf{r},t)$, which is used to generate the balance equations, i.e.,

$$D\mathbf{A} = D(\bar{\mathbf{X}}d\tau_0) = D(\bar{\mathbf{X}})d\tau_0 + \bar{\mathbf{X}}D(d\tau_0) = (D\bar{\mathbf{X}} + \bar{\mathbf{X}}\boldsymbol{\nabla}\cdot\mathbf{u})d\tau_0, \tag{17}$$

where $\mathbf{u} = d\mathbf{r}/dt$ and $D(d\tau_0) = d\tau_0\boldsymbol{\nabla}\cdot\mathbf{u}\cdot\bar{\mathbf{X}}$ is generally dependent on physical properties. For example, the linear momentum $\rho\mathbf{u}$ is changed by the body and surface forces [38]. Therefore, without losing generality, we assume

$$D\mathbf{A} = \mathbf{B}d\tau_0, \tag{18}$$

where $\mathbf{B}$ is a undermined vector. Then, if $\mathbf{B}$ is given, from Eqs. (17) and (18) we obtain a balance equation for property $\bar{\mathbf{X}}$, given by

$$D\bar{\mathbf{X}} + \bar{\mathbf{X}}\boldsymbol{\nabla}\cdot\mathbf{u} = \mathbf{B}. \tag{19}$$

$\mathbf{B}$ can be determined from the balance equations of the discrete system according to Eq. (A18) in the Appendix. So, we finally obtain the balance equations for the continuum system corresponding to the discrete system considered,

$$D(\bar{\mathbf{X}}) + \bar{\mathbf{X}}\boldsymbol{\nabla}\cdot\mathbf{u} = \boldsymbol{\nabla}\cdot\mathbf{H} + \mathbf{P} + \mathbf{G}. \tag{20}$$

As a special case of Eq. (20), the balance equations of mass, linear momentum, angular momentum, and energy are, respectively,

$$D(\rho) + \rho\boldsymbol{\nabla}\cdot\mathbf{u} = 0, \tag{21}$$

$$D(\rho\mathbf{u}) + \rho\mathbf{u}\boldsymbol{\nabla}\cdot\mathbf{u} = \boldsymbol{\nabla}\cdot\mathbf{T} + \rho\mathbf{g}, \tag{22}$$

$$D(\rho\mathbf{l}\cdot\boldsymbol{\omega}) + \rho\mathbf{l}\cdot\boldsymbol{\omega}\cdot\mathbf{u} = \boldsymbol{\nabla}\cdot\mathbf{M} + \mathbf{M}', \tag{23}$$

$$D(\rho E) + \rho E\boldsymbol{\nabla}\cdot\mathbf{u} = \boldsymbol{\nabla}\cdot(\mathbf{T}\cdot\mathbf{u} + \mathbf{M}\cdot\boldsymbol{\omega}) + \boldsymbol{\nabla}\cdot\mathbf{q}^E + \rho\mathbf{g}\cdot\mathbf{u} + \rho h, \tag{24}$$

where

$$\mathbf{T} = -\int_{T_t}\sum_i h_i m_i\mathbf{v}_i'\otimes\mathbf{v}_i'ds + \int_{T_t}\sum_i\sum_{j>i} g_{ij}\mathbf{d}_{ij}\otimes\mathbf{f}_{ij}ds + \int_{T_t}\sum_i g_i^b\mathbf{d}_i^b\otimes\mathbf{f}_i^b ds, \tag{25}$$

$$\mathbf{M} = -\int_{T_t}\sum_i h_i\mathbf{v}_i'\otimes(\mathbf{l}_i\cdot\boldsymbol{\omega}_i)ds + \frac{1}{2}\int_{T_t}\sum_i\sum_{j>i} g_{ij}\mathbf{d}_{ij}\otimes(\mathbf{m}_{ij} - \mathbf{m}_{ji})ds + \int_{T_t}\sum_i g_i^b\mathbf{d}_i^b\otimes\mathbf{m}_i^b ds, \tag{26}$$

$$\mathbf{M}' = \frac{1}{2}\int_{T_t}\sum_i\sum_{j>i}(\mathbf{m}_{ij} + \mathbf{m}_{ji})(h_i + h_j)ds, \tag{27}$$

$$\mathbf{q}^E = -\frac{1}{2}\int_{T_t}\sum_i h_i m_i\mathbf{v}_i'\otimes\mathbf{v}_i'\cdot\mathbf{v}_i'ds - \frac{1}{2}\int_{T_t}\sum_i h_i\mathbf{v}_i'\otimes(\mathbf{l}_i\cdot\boldsymbol{\omega}_i)\cdot(\boldsymbol{\omega}_i' - \boldsymbol{\omega})ds - \int_{T_t}\sum_i h_i\varepsilon_i\mathbf{v}_i'ds + \int_{T_t}\sum_i\sum_{j>i} g_{ij}[W_{ij} + Q_{ij} - \mathbf{f}_{ij}\cdot\mathbf{u}$$

$$-\tfrac{1}{2}(\mathbf{m}_{ij} - \mathbf{m}_{ji})\cdot\boldsymbol{\omega}]\mathbf{d}_{ij}ds + \int_{T_t}\sum_i g_i^b(W_i^b + Q_i^b - \mathbf{f}_i^b\cdot\mathbf{u} - \mathbf{m}_i^b\cdot\boldsymbol{\omega})\mathbf{d}_i^b ds, \tag{28}$$

$$h = \frac{1}{\rho}\int_{T_t}\sum_i H_i h_i dt. \tag{29}$$

It is evident from Eqs. (21)–(24) that the balance equations of mass and linear momentum are the same as those in the classical continuum mechanics, and an extra equation is used to describe the rotation of the independent particles. The derivation of variable $\mathbf{B}$ in the Appendix suggests that these balances are automatically maintained in the whole domain including regions adjacent to physical boundaries. This is important to overcome the problems associated with the pre-

vious averaging methods. For example, Barbic's method cannot apply to regions close to physical boundaries [32]. Luding *et al.* [34] observed imbalance near a boundary due to unknown missing contributions in their averaging. In fact, it can be shown that the equations developed by Barbic [32] are the special case of the above equations when the presence of physical boundaries is ignored. Table I lists the physical meaning of the key macroscopic quantities involved. They

can be determined from the microscopic quantities in the balance equations of particles by Eqs. (9)–(13) and (25)–(29). In other words, the macroscopic variables in the continuum approach can be directly linked to the microscopic variables in the discrete approach.

C. Weighting function

Strictly speaking, the macroscopic quantities are not uniquely determined from the microscopic quantities for a given flow system because of the uncertainty with the weighting function $h(\mathbf{r},t)$. Therefore, the selection of a proper weighting function is important in applying the equations formulated above. In general, besides the condition of normalization, the weighting function $h(\mathbf{r},t)$ should satisfy the following three conditions:

$$\text{(i)} \quad h(\mathbf{r},t) \in C^r(R^4) \quad (r \geq 1),$$

$$\text{(ii)} \quad h(\mathbf{r},t) \begin{cases} >0, & (\mathbf{r},t) \in \hat{\Omega} = \Omega \backslash \partial\Omega \\ =0, & (\mathbf{r},t) \in R^4 \backslash \hat{\Omega}, \end{cases}$$

and (iii) $h(\mathbf{r},t)$ decreases monotonically in Ω with increasing $|\mathbf{r}|$ and $|t|$. The first condition is necessary in the derivation of the balance equations and it also ensures that the average properties smoothly vary in a considered domain. The second and third conditions guarantee that the contribution of different particles to a probe point or the contribution of different time to a probe time is different. They represent a physical consideration that the contribution of the particles near a probe point or time close to a probe time should be larger, and particles or time far away from a probe point or a probe time do not have any contribution.

The need to find out a suitable weighting function has been noticed in the literature [35,37]. We here recommend the use of a weighting function which arises from the so-called Johnson's S_B distribution function [39]. This function has been widely used in engineering practice, e.g., in the mathematical representation of particle size distribution of granular materials where distribution transformation is often required (see Ref. [40], for example). For the present application, the weighting function is given by

$$h(\mathbf{r},t) = f(t)g(r), \tag{30}$$

where $r = |\mathbf{r}|$, and $f(t)$ is the simplified S_B distribution function explicitly written as

$$f(t) = \begin{cases} \dfrac{\sigma_t}{\sqrt{2\pi}} \dfrac{2L_t}{(L_t^2 - t^2)} \exp\left(-\dfrac{\sigma_t^2}{2} \ln^2 \dfrac{L_t + t}{L_t - t} \right), & |t| < L_t \\ 0, & |t| \geq L_t, \end{cases} \tag{31}$$

where L_t, σ_t are the distribution parameters. On the other hand, $g(r)$ is an extension of the univariate distribution (31) to three variants, so that,
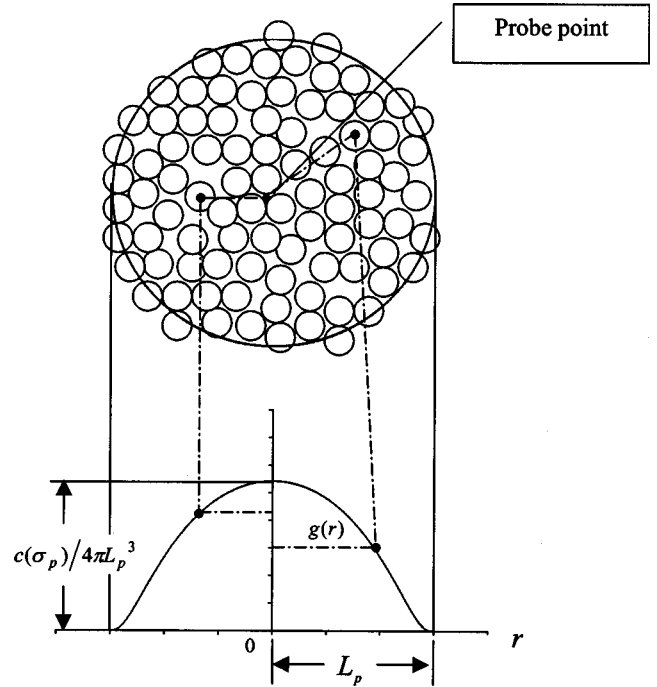
FIG. 2. Concept of weighting, when coupled with Johnson's S_B distribution function, for space averaging (the same idea applied to time averaging).

$$g(r) = \begin{cases} \dfrac{c}{4\pi L_p(L_p^2 - r^2)} \exp\left(-\dfrac{\sigma_p^2}{2} \ln^2 \dfrac{L_p + r}{L_p - r} \right), & r < L_p \\ 0, & r \geq L_p, \end{cases} \tag{32}$$

where L_p, σ_p are the distribution parameters, $c = c(\sigma_p)$ is the normalized constant of the distribution function $g(r)$, which is expressed as

$$c(\sigma_p) = \left[\int_0^1 \frac{r^2}{1 - r^2} \exp\left(-\frac{\sigma_p^2}{2} \ln^2 \frac{1+r}{1-r} \right) dr \right]^{-1}. \tag{33}$$

The above integral can be calculated numerically. It can be shown that $c(\sigma_p)$ is a monotonic function of σ_p. The above distribution functions are smooth in the entire space, and decrease monotonically with increasing $|\mathbf{r}|$ or $|t|$, as typically illustrated in Fig. 2.

This weighting function is thus far the only one that satisfies fully the requirements mentioned above. An open question with the weighting function is the selection of the parameters, which is important in our setup because L_t or L_p determines the amount of the contributing particles to a probe point, whereas σ_t or σ_p controls the magnitude of weighting average to every particle. On the other hand, one of the main advantages of using this weighting function is that the size of the cell is not necessarily increased for the continuity of resulting average quantities [37]. This is very useful since at this stage of development, almost all DEM

TABLE II. Parameters used in the present DEM simulation.

Quantity	Value	Units
Hopper diameter	30.0	d
Orifice diameter	8.0	d
Number of particles	24 000	
Friction coefficient (particle-particle)	0.6	
Friction coefficient (particle-wall)	0.3	
Rolling friction coefficient (particle-particle or particle-wall)	0.001	d
Young's modulus of particle or wall	50 000	mg/d^2
Poisson ratio of particle or wall	0.3	
Normal damping ratio (particle-particle or particle-wall)	0.1	
Tangential damping ratio (particle-particle or particle-wall)	0.3	
Time step	0.001	$\sqrt{d/g}$
Time to start discharging	80.0	$\sqrt{d/g}$

simulations have to be carried out with a relatively small number of particles because of the limited computing capability.

III. APPLICATION TO A HOPPER FLOW

A. DEM simulation

Understanding and modeling the granular flow in a hopper flow is of great importance and has been a research focus worldwide for years. The dynamic behavior of hopper flow is very complicated because all the flow regimes mentioned above may coexist. The continuum models proposed thus far, including those from either the plasticity model or the kinetic theory, cannot satisfactorily apply to this flow [31]. Current experimental technique cannot generate much information about the internal properties, e.g., stress distributions. As shown in this section, the combination of the discrete approach and the averaging technique proposed here provides an effective way to study the macroscopic behavior.

We consider the granular flow in a cylindrical 3D hopper with flat bottom. Discrete simulation is performed by means of a modified DEM. The simulation technique has been well demonstrated in our previous work [41,42], which is essentially the same as that originally proposed by Cundall [10] but modified by incorporating a rolling friction model. Table II lists the physical parameters used in this work. Note that the long-range forces such as van der Waals and electrostatic forces are ignored in the present work which deals with the flow of relatively large particles. The procedure used in the simulation is as follows. First, 24 000 monosized spherical particles (particle diameter $d=3$ mm; particle density $\rho_p = 2500$ kg/m^3) are randomly generated in the hopper without overlap. These particles are then allowed to settle onto the hopper to form a packing, and finally discharged under gravity when the hopper outlet is removed, as shown in Fig. 3.

B. Quantification of continuum variables

We calculate, based on the data generated from the above DEM simulation, the mass density field, the velocity field, the stress, and couple stress fields by using the averaging

method proposed above. Because of the relatively perfect axial symmetry, this three-dimensional flow problem is here examined on a sectional plane. Thus, the velocity has only two components, the stress tensor and the couple stress tensor each have four components. The values of all computed quantities at every probe point, which are expressed by the cylindrical coordinates, are the average values of the two symmetrical points in the plane. Therefore, only the values in half the plane are shown. The mass density, the velocity, the stress tensor, and the couple stress tensor are non-dimensionalized as $\bar{\rho}(\bar{\mathbf{r}},\bar{t})=[6/(\pi\rho_p)]\rho(\mathbf{r},t)$, $\bar{\mathbf{u}}(\bar{\mathbf{r}},\bar{t})=(gd)^{-1/2}\mathbf{u}(\mathbf{r},t)$, $\bar{\mathbf{T}}(\bar{\mathbf{r}},\bar{t})=[6/(\pi\rho_p dg)]\mathbf{T}(\mathbf{r},t)$ and $\bar{\mathbf{M}}(\bar{\mathbf{r}},\bar{t})=[6/(\pi\rho_p d^2 g)]\mathbf{M}(\mathbf{r},t)$, respectively. As discussed elsewhere [37], the macroscopic quantities calculated will depend on the parameters in the weighting function, i.e., the cell size and the weighting within the cell, although the resulting trends are consistent. Their proper selection is still open for research. This problem also exists for other averaging methods, as, for example, shown by Lätzel, Luding, and Herrmann [22]. In this work, parameters σ_t, σ_p, L_t, and L_p are, respectively, given as $\sigma_t=\sigma_p=1.0$ and $L_t=L_p=4.0$. In all figures, $\bar{r}$ denotes the distance from a probe point to the central axis of the hopper, while $\bar{z}$ denotes the height of a probe point above the bottom of the hopper.

(a)   (b)
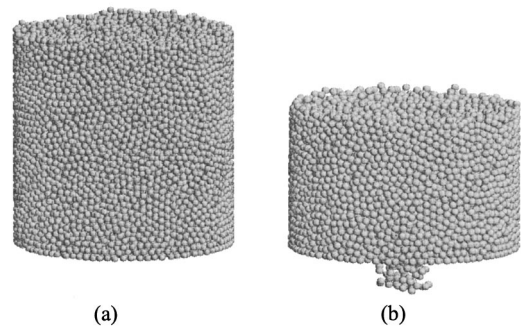
FIG. 3. Snapshots showing the discharging process of hopper flow when: (a) $\bar{t}=80$ (time to start discharging); and (b) $\bar{t}=240\sqrt{d/g}$.
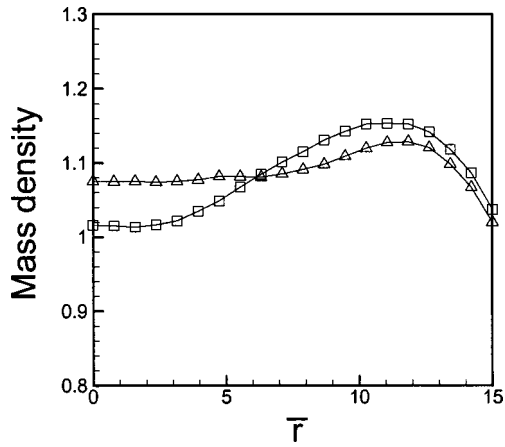
FIG. 4. Radial distribution of mass density (of units $\pi \rho_p/6$) when $\bar{t}=240.0\sqrt{d/g}$: $\square$, $\bar{z}=4.0$; $\triangle$, $\bar{z}=8.0d$.

Figure 4 shows the distribution of the mass density at two different heights at a given time. It can be seen that the mass density increases gradually to a maximum and then decreases with increasing radius; the variation is small in the central region and significant in the region adjacent to the wall. It also varies with height $\bar{z}$ because of the effect of the bottom wall; the change is more significant when $\bar{z}$ is low. To be more quantitative, we calculate packing density c at several typical points, and obtain $c=0.532$ at $\bar{r}=0.0$, $c=0.543$ at $\bar{r}=15.0$, and $c=0.604$ at the peak when $\bar{z}=4.0$; and $c=0.563$ at $\bar{r}=0.0$, $c=0.534$ at $\bar{r}=15.0$, and $c=0.59$ at the peak when $\bar{z}=8.0$. The observed maximum packing density $c=0.604$ is close to that obtained under conditions of loose random packing [42]. The decreased density in the region close to the wall is mainly due to the effect of wall or physical boundaries [43]. On the other hand, the decrease in mass density in the central region is due to the dilatancy of granular materials. Often a low mass density corresponds to a high velocity [44,45]. This is indeed the case when examining the velocity distributions at the two heights as shown in Fig. 5. Two velocity components, i.e., vertical and horizontal velocities, are considered. It can be seen that the magnitude of the vertical velocity decreases with increasing radius in the central region and is relatively insignificant in the region close to the wall. The variation of horizontal velocity is also largely limited to the central region, with its magnitude increasing from zero to a maximum and then decreasing with
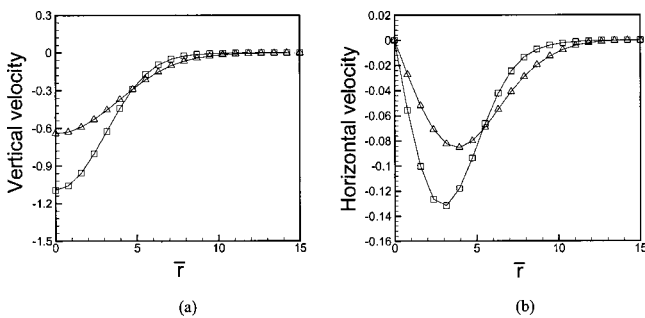
FIG. 5. Radial velocity distribution (units for velocity are $\sqrt{gd}$) when $\bar{t}=240.0\sqrt{d/g}$: $\square$, $\bar{z}=4.0$; $\triangle$, $\bar{z}=8.0d$.
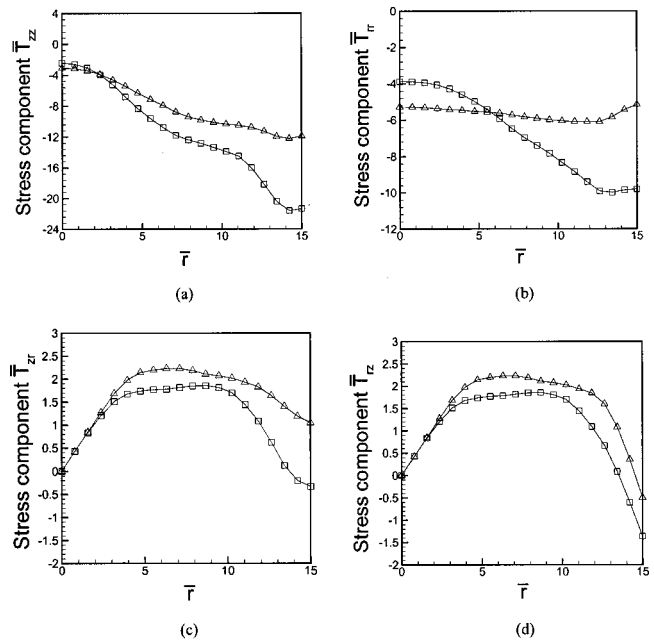
FIG. 6. Radial stress distribution (units for stress are $\pi \rho_p dg/6$) when $\bar{t}=240.0\sqrt{d/g}$: $\square$, $\bar{z}=4.0$; $\triangle$, $\bar{z}=8.0d$.

increasing radius. The lower the position, the more significant the variation for both velocity components. However, because the magnitude of the vertical component is much larger than that of horizontal component, the vertical movement of particles is dominant. These results are qualitatively in agreement with the experimental observations [45].

Figure 6 shows the internal stress distributions of the hopper flow when $\bar{z}=4.0$ and 8.0. It can be observed from Figs. 6(a) and 6(b) that the magnitudes of the two normal stresses $\bar{T}_{zz}$ and $\bar{T}_{rr}$ increase with $\bar{r}$ except for a small increase close to the wall. On the other hand, Figs. 6(c) and 6(d) show that the two shear stresses $\bar{T}_{rz}$ and $\bar{T}_{zr}$ are almost identical in the central region, which is in agreement with the previous continuum description of hopper flow [45]. However, the two shear stresses are different in the region adjacent to the wall.

Figure 7 shows the couple stress distributions of the hopper flow at the same heights. The results indicate that under the present simulation conditions, the change in the four components is very small and can be reasonably ignored, although the small variation observed may result in some fluctuation in flow behavior. However, this consideration is not applicable to $\bar{M}_{rr}$ and $\bar{M}_{rz}$ in the region adjacent to the wall. Both stress components vary significantly in that region. Therefore, all the results in Figs. 4–7 point to one important fact: the presence of physical boundaries will affect both microscopic and macroscopic quantities related to granular flow and must be properly considered.

CONCLUSIONS

An averaging method has been developed to obtain the macroscopic quantities in the continuum description of granular flow from the microscopic quantities generated by DEM-based discrete simulation. Compared to the other
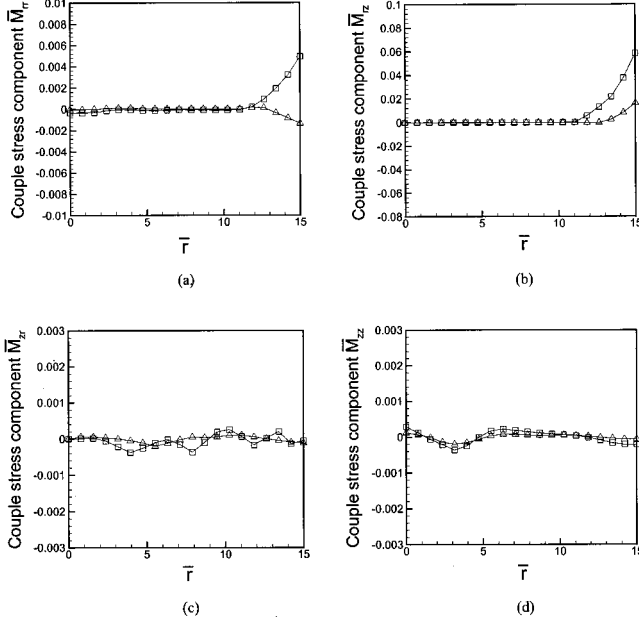
FIG. 7. Radial distribution of couple stress (of units $\pi\rho_p d^2 g/6$) when $\bar{t}=240.0\sqrt{d/g}$: $\square$, $\bar{z}=4.0$; $\triangle$, $\bar{z}=8.0d$.

methods proposed in the literature, it has advantages of being applicable to all flow regimes, and to granular flows with or without the effect of physical boundaries. Moreover, smooth variation in the resultant macroscopic quantities can be ensured even though a simulation may be carried out with a limited number of particles. The method will provide an effective way to study the fundamentals governing granular flow, which is otherwise difficult to obtain with the current experimental techniques.

The application of the method is demonstrated in the calculation of velocity and stress fields of a hopper flow. Preliminary analysis of the results indicates that the mass density, velocity, stress, and couple stress distributions are qualitatively comparable with those in the conventional continuum description in the region far from the physical boundary; the presence of physical boundaries will significantly affect these properties. Further studies are being conducted in order to develop a better understanding of this important flow system.

APPENDIX: DERIVATION OF EQUATION TO CALCULATE B IN EQ. (19)

For simplicity, let $\mathbf{X}_i = \mathbf{X}_i(s)$, $\mathbf{v}_i = \mathbf{v}_i(s)$ in the following derivation. According to the definition of material derivative, we have

$$D(\bar{\mathbf{X}}) + \bar{\mathbf{X}}\nabla\cdot\mathbf{u} = \partial_t(\bar{\mathbf{X}}) + \nabla\cdot(\mathbf{u}\otimes\bar{\mathbf{X}}). \tag{A1}$$

Considering $\mathbf{u} = \mathbf{v}_i - \mathbf{v}_i'$ and from Eq. (6),

$$\partial_t(\bar{\mathbf{X}}) = \int_{T_t}\sum_i \partial_t h_i \mathbf{X}_i ds, \tag{A2}$$

$$\nabla\cdot(\mathbf{u}\otimes\bar{\mathbf{X}}) = \int_{T_t}\sum_i (\partial_r h_i\cdot\mathbf{v}_i)\mathbf{X}_i ds - \nabla\cdot\int_{T_t}\sum_i h_i\mathbf{v}_i'\otimes\mathbf{X}_i ds. \tag{A3}$$

Substituting Eqs. (A2) and (A3) into Eq. (A1) and noting $\partial_r h_i = -\partial_{r_i} h_i$, $\partial_t h_i = -\partial_s h_i$, we can obtain

$$D(\bar{\mathbf{X}}) + \bar{\mathbf{X}}\nabla\cdot\mathbf{u} = \int_{T_t}\sum_i h_i\frac{d\mathbf{X}_i}{ds}ds - \nabla\cdot\int_{T_t}\sum_i h_i\mathbf{v}_i'\otimes\mathbf{X}_i ds. \tag{A4}$$

Substituting Eq. (5) into the above equation gives

$$D(\bar{\mathbf{X}}) + \bar{\mathbf{X}}\nabla\cdot\mathbf{u} = \int_{T_t}\sum_i\sum_j h_i\mathbf{P}_{ij}ds + \int_{T_t}\sum_i h_i\mathbf{B}_i ds$$
$$+ \int_{T_t}\sum_i h_i\mathbf{G}_i ds - \nabla\cdot\int_{T_t}\sum_i h_i\mathbf{v}_i'\otimes\mathbf{X}_i ds. \tag{A5}$$

Comparing Eq. (A5) and Eq. (19) yields

$$\mathbf{B} = \int_{T_t}\sum_i\sum_j h_i\mathbf{P}_{ij}ds + \int_{T_t}\sum_i h_i\mathbf{B}_i ds$$
$$+ \int_{T_t}\sum_i h_i\mathbf{G}_i ds - \nabla\cdot\int_{T_t}\sum_i h_i\mathbf{v}_i'\otimes\mathbf{X}_i ds. \tag{A6}$$

Then, we modify the treatment of Babic [32] to simplify this expression. First, we decompose the first term of the right-hand side of Eq. (A6) to two terms,

$$\int_{T_t}\sum_i\sum_j h_i\mathbf{P}_{ij}ds = \frac{1}{2}\int_{T_t}\sum_i\sum_{j>i}(h_i-h_j)(\mathbf{P}_{ij}-\mathbf{P}_{ji})ds$$
$$+ \frac{1}{2}\int_{T_t}\sum_i\sum_{j>i}(h_i+h_j)(\mathbf{P}_{ij}+\mathbf{P}_{ji})ds$$
$$= \mathbf{P}_0 + \mathbf{P}_1, \tag{A7}$$

where

$$\mathbf{P}_0 = \frac{1}{2}\int_{T_t}\sum_i\sum_{j>i}(h_i-h_j)(\mathbf{P}_{ij}-\mathbf{P}_{ji})ds, \tag{A8}$$

$$\mathbf{P} = \frac{1}{2}\int_{T_t}\sum_i\sum_{j>i}(h_i+h_i)(\mathbf{P}_{ij}+\mathbf{P}_{ji})ds. \tag{A9}$$

Depending to the positions of particles i and j, there are four cases: (1) $\mathbf{r}_i-\mathbf{r}\in\Omega_p$, $\mathbf{r}_j-\mathbf{r}\in\Omega_p$; (2) $\mathbf{r}_i-\mathbf{r}\in\Omega_p$, $\mathbf{r}_j-\mathbf{r}\notin\Omega_p$; (3) $\mathbf{r}_i-\mathbf{r}\notin\Omega_p$, $\mathbf{r}_j-\mathbf{r}\in\Omega_p$; (4) $\mathbf{r}_i-\mathbf{r}\notin\Omega_p$, $\mathbf{r}_j-\mathbf{r}\notin\Omega_p$. For the first case, $h(\mathbf{r}_i-\mathbf{r}, s-t)>0$, $h(\mathbf{r}_j-\mathbf{r}, s-t)>0$. For the second case, $h(\mathbf{r}_i-\mathbf{r}, s-t)>0$, $h(\mathbf{r}_j-\mathbf{r}, s-t)=0$, thus, because $h(\mathbf{r}_j'-\mathbf{r}, s-t)=h(\mathbf{r}_j-\mathbf{r}, s-t)=0$,

we can replace $h(\mathbf{r}_j - \mathbf{r}, \, s-t)$ in the right-hand side of Eq. (A8) with $h(\mathbf{r}_j' - \mathbf{r}, \, s-t)$, where $\mathbf{r}_j'$ is the point of intersection of the line connecting the centers of mass of particles i and j and the boundary $\partial\Omega_p$ of domain Ω_p. Similar to (2), for the third case, $h(\mathbf{r}_j - \mathbf{r}, \, s-t) = 0$, $h(\mathbf{r}_j - \mathbf{r}, \, s-t) > 0$, so $h(\mathbf{r}_i - \mathbf{r}, \, s-t)$ can be replaced with $h(\mathbf{r}_i' - \mathbf{r}, \, s-t)$. Finally, for the fourth case, particles i and j have no contribution to $\mathbf{P}_0$; consequently, this case is neglected in the following analysis. Let $\bar{\mathbf{r}}_j = \mathbf{r}_j$ ($\bar{\mathbf{r}}_i = \mathbf{r}_i$) if $\mathbf{r}_j - \mathbf{r} \in \Omega_p$ ($\mathbf{r}_i - \mathbf{r} \in \Omega_p$); otherwise, $\bar{\mathbf{r}}_j = \mathbf{r}_j'$ ($\bar{\mathbf{r}}_i = \mathbf{r}_i'$). Then, Eq. (A8) can be rewritten as

$$\mathbf{P}_0 = \frac{1}{2} \int_{T_t} \sum_i \sum_{j>i} [h(\bar{\mathbf{r}}_i - \mathbf{r}, \, s-t) - h(\bar{\mathbf{r}}_j - \mathbf{r}, \, s-t)]$$
$$\times (\mathbf{P}_{ij} - \mathbf{P}_{ji}) ds. \qquad (A10)$$

Since

$$h(\bar{\mathbf{r}}_i - \mathbf{r}, \, s-t) - h(\bar{\mathbf{r}}_j - \mathbf{r}, \, s-t)$$
$$= -\int_0^1 \frac{d}{dr} h(\bar{\mathbf{r}}_i + r\mathbf{d}_{ij} - \mathbf{r}, \, s-t) dr$$
$$= \int_0^1 \frac{\partial}{\partial \mathbf{r}} h(\bar{\mathbf{r}}_i + r\mathbf{d}_{ij} - \mathbf{r}, \, s-t) \cdot \mathbf{d}_{ij} dr, \qquad (A11)$$

where $\mathbf{d}_{ij} = \bar{\mathbf{r}}_j - \bar{\mathbf{r}}_i$, substituting Eq. (A11) into Eq. (A10) gives

$$\mathbf{P}_0 = \nabla \cdot \left\{ \frac{1}{2} \int_{T_t} \sum_i \sum_{j>i} \left[\int_0^1 h(\bar{\mathbf{r}}_i + r\mathbf{d}_{ij} - \mathbf{r}, \, s-t) dr \right] \mathbf{d}_{ij} \right.$$
$$\left. \otimes (\mathbf{P}_{ij} - \mathbf{P}_{ji}) ds \right\}. \qquad (A12)$$

In the present study, it is assumed that, compared to the physical boundary, the sizes of particles are so small that the contact between particle i and a boundary is equivalent to the contact between the particle and a spherical particle with enough large mass and diameter. Therefore, the interaction between a particle and boundary belongs to the second or

fourth case. Similarly to the above treatment about the interaction between particles, we can transfer the second term of the right-hand side of Eq. (A6) to

$$\int_{T_t} \sum_i h_i \mathbf{B}_i ds = \nabla \cdot \left\{ \int_{T_t} \sum_i \left[\int_0^1 h(\mathbf{r}_i + r\mathbf{d}_i^b - \mathbf{r}, \, s-t) dr \right] \mathbf{d}_i^b \right.$$
$$\left. \otimes \mathbf{B}_i ds \right\}. \qquad (A13)$$

If particle i contacts a physical boundary, $\mathbf{d}_i^b$ is the ray from the center of mass of particle i to a point on boundary $\partial\Omega_p$ of domain Ω_p, via a point on the physical boundary, and perpendicular to the tangential plane of the point; otherwise, $\mathbf{d}_i^b = \mathbf{0}$. For convenience, let

$$\mathbf{H} = -\int_{T_t} \sum_i h_i \mathbf{v}_i' \otimes \mathbf{X}_i ds$$
$$+ \frac{1}{2} \int_{T_t} \sum_i \sum_{j>i} g_{ij} \mathbf{d}_{ij} \otimes (\mathbf{P}_{ij} - \mathbf{P}_{ji}) ds$$
$$+ \int_{T_t} \sum_i g_i^b \mathbf{d}_i^b \otimes \mathbf{B}_i ds, \qquad (A14)$$

$$\mathbf{G} = \int_{T_t} \sum_i h_i \mathbf{G}_i ds, \qquad (A15)$$

where

$$g_{ij} = \int_0^1 h(\bar{\mathbf{r}}_i + r\mathbf{d}_{ij} - \mathbf{r}, \, s-t) dr, \qquad (A16)$$

$$g_i^b = \int_0^1 h(\mathbf{r}_i + r\mathbf{d}_i^b - \mathbf{r}, \, s-t) dr. \qquad (A17)$$

Then, from Eqs. (A6), (A7), and (A12)–(A15), we can obtain the expression of $\mathbf{B}$, given by

$$\mathbf{B} = \nabla \cdot \mathbf{H} + \mathbf{P} + \mathbf{G}. \qquad (A18)$$

[1] H. M. Jaeger, S. R. Nagel, and R. P. Behringer, Rev. Mod. Phys. **68**, 1259 (1996).
[2] P. G. de Gennes, Rev. Mod. Phys. **71**, S374 (1999).
[3] S. F. Edwards and D. V. Grinev, Physica A **302**, 162 (2001).
[4] M. Oda and K. Iwashita, *Mechanics of Granular Materials* (A. A. Balkema, Rotterdam, 1999).
[5] W. Powrie, *Soil Mechanics: Concepts and Applications* (E & FN Spon, London, 1997).
[6] A. J. M. Spencer, J. Mech. Phys. Solids **12**, 337 (1964).
[7] C. K. K. Lun, S. B. Savage, D. J. Jeffrey, and N. Chepurniy, J. Fluid Mech. **140**, 223 (1984).
[8] C. S. Campbell, Annu. Rev. Fluid Mech. **22**, 57 (1990).
[9] P. C. Johnson and R. Jackson, J. Fluid Mech. **176**, 67 (1987).
[10] P. A. Cundall, Proc. Symp. Int. Soc. Rock Mech **2**, 129 (1971).
[11] P. A. Cundall and O. D. L. Strack, Geotechnique **29**, 47 (1979).
[12] Powder Technol. **109**, 1 (2000), special issue on numerical simulation of discrete particle systems, edited by C. Thornton.
[13] A. Drescher and G. de Josselin de Jong, J. Mech. Phys. Solids **20**, 337 (1972).
[14] L. Rothenburg and A. P. S. Selvadurai, in *Proceedings of the International Symposium on the Mechanical Behavior of Structured Media*, edited by A. P. S. Selvadurai (Ottawa, Canada, 1981), p. 469.
[15] J. Christoffersen, M. M. Mehrabadi, and S. Nemat-Nasser, ASME J. Appl. Mech. **48**, 339 (1981).
[16] K. Kanatani, Powder Technol. **28**, 167 (1981).
[17] R. J. Bathurst and L. Rothenburg, ASME J. Appl. Mech. **55**, 17 (1988).
[18] N. P. Kruyt and L. Rothenburg, ASME J. Appl. Mech. **118**, 706 (1996).

[19] K. Bagi, Mech. Mater. **22**, 165 (1996).

[20] C. L. Liao, T. P. Chang, D. H. Young, and C. S. Chang, Int. J. Solids Struct. **34**, 4087 (1997).

[21] N. P. Kruyt and L. Rothenburg, Int. J. Eng. Sci. **36**, 1127 (1998).

[22] M. Lätzel, S. Luding, and H. J. Herrmann, Granular Matter **2**, 123 (2000).

[23] M. Lätzel, S. Luding, and H. J. Herrmann, in *Continuous and Discontinuous Modelling of Cohesive-Frictional Materials*, edited by P. A. Vermeer, S. Diebels, W. Ehlers, H. J. Herrmann, S. Luding, and E. Ramm (Springer, Berlin, 2001), pp. 215–230.

[24] S. Luding, in *Powders and Grains*, edited by Y. Kishino (A. A. Balkema, Tokyo, 2001), pp. 141–148.

[25] O. R. Walton and R. L. Braun, J. Rheol. **30**, 949 (1986).

[26] O. R. Walton and R. L. Braun, Acta Mech. **63**, 73 (1986).

[27] Y. Zhang and C. S. Campbell, J. Fluid Mech. **237**, 541 (1992).

[28] C. S. Campbell, J. Fluid Mech. **247**, 111 (1993).

[29] C. S. Campbell, J. Fluid Mech. **247**, 137 (1993).

[30] P. A. Langston, U. Tüzün, and D. M. Heyes, Powder Technol. **85**, 153 (1995).

[31] A. V. Potapov and C. S. Campbell, Phys. Fluids **8**, 2884 (1996).

[32] M. Babic, Int. J. Eng. Sci. **35**, 523 (1997).

[33] M. Babic, Phys. Fluids **9**, 2486 (1997).

[34] S. Luding, M. Lätzel, W. Volk, S. Diebels, and H. J. Herrmann, Comput. Methods Appl. Mech. Eng. **191**, 21 (2001).

[35] B. J. Glasser and I. Goldhirsch, Phys. Fluids **13**, 407 (2001).

[36] I. Goldhirsch and C. Goldenberg, e-print cond-mat/02033060.

[37] H. P. Zhu and A. B. Yu, Bulk Solids Handling **20**, 53 (2001).

[38] S. B. Savage, J. Fluid Mech. **377**, 1 (1998).

[39] N. L. Johnson, Biometrika **36**, 149 (1949).

[40] A. B. Yu and N. Standish, Powder Technol. **62**, 101 (1990).

[41] Y. C. Zhou, B. D. Wright, R. Y. Yang, B. H. Xu, and A. B. Yu, Physica A **269**, 536 (1999).

[42] R. Y. Yang, R. P. Zou, and A. B. Yu, Phys. Rev. E **62**, 3900 (2000).

[43] R. P. Zou and A. B. Yu, Chem. Eng. Sci. **50**, 1504 (1995).

[44] S. Humby, U. Tüzün, and A. B. Yu, Chem. Eng. Sci. **53**, 483 (1998).

[45] J. P. K. Seville, U. Tüzün, and R. Clift, *Processing of Particulate Solids* (Blackie Academic & Professional, London, 1997).